infrastructures

MDPI

Article

Parametric Analysis in the Optimization Design of Composite Cellular Beams †

Maria Célia Loss Brandão [1], Lorena Yepes-Bellver [2], Moacir Kripka [3] and Élcio Cassimiro Alves [1,*]

[1] Department of Civil Engineering, Federal University of Espírito Santo, Vitória 29075-910, ES, Brazil; maria.l.brandao@edu.ufes.br
[2] ICITECH. Department of Structural Mechanics and Theory of Structures, Universitat Politècnica de València (UPV), 46022 Valencia, Spain; loyebel@upvnet.upv.es
[3] Department of Civil Engineering, University of Passo Fundo, Passo Fundo 99001-970, RS, Brazil; mkripka@upf.br
* Correspondence: elcio.alves@ufes.br

† This paper is an extended version of the paper Published: Multi-Objective Optimization of Steel and Concrete Composite Cellular Beams. In Proceedings of the CILAMCE 2025 XLVI Ibero-Latin American Congress on Computational Methods in Engineering, Vitória, ES, Brazil, 24–27 November 2025.

Abstract

This study aims to present a parametric analysis in the optimization problem for steel-concrete composite cellular beams with steel deck slabs. A comparative analysis was carried out considering two scenarios, namely, (i) in the first scenario, the slab span and applied loads were varied, adopting slab configurations from a manufacturer's catalog for spans of 10 m to 20 m with a step of 2.5 m; (ii) in the second scenario, the same span and loading conditions were considered; however, slab optimization was performed by introducing reinforcement in order to evaluate the resulting impacts on the structural design. In both analyzed scenarios, the objective function was defined as the composite system's CO_2 emissions. The design constraints were defined based on literature recommendations, and to solve the optimization problem, the Particle Swarm Optimization (PSO) algorithm was also adopted. The results demonstrate that the PSO algorithm was effective in identifying optimal solutions and that the introduction of slab reinforcement, combined with optimal design, led to CO_2 emission reductions of up to 25% at the highest load levels analyzed.

Keywords: composite cellular beams; CO_2 emission; particle swarm optimization; steel-deck composite slab

1. Introduction

Since the Industrial Revolution, the exploitation of natural resources has increased dramatically, driving technological and economic growth. This has improved living standards through advances in infrastructure, healthcare, and housing. However, the development model has relied on excessive use of raw materials and energy, ignoring ecological limits. The rapid expansion of factories and industrial cities, along with a capital-driven production logic and the growth of the construction industry, has led to severe environmental impacts, including pollution and greenhouse gas emissions. The construction sector is a major contributor, responsible for significant resource extraction, waste, and emissions. According to the Global Status Report for Buildings and Construction 2024/2025 [1], the sector accounts for 32% of global energy consumption and 34% of CO_2 emissions, with cement and steel accounting for 18%. This highlights the urgent need to address construction's environmental impact and pursue sustainable industrial development. Within this

Check for updates

Academic Editor: Alessio Cascardi

Received: 11 March 2026
Revised: 1 April 2026
Accepted: 9 April 2026
Published: 13 April 2026

framework, composite steel structures emerge as an alternative by reducing the use of steel and concrete, two materials that generate the highest CO_2 emissions in the construction sector during production. In particular, cellular beams further reduce this by enhancing material efficiency, enabling longer spans without compromising structural performance.

The application of optimization techniques in steel–concrete composite systems has been widely explored over the past decades, as evidenced by the works of Tormen et al. [2] (composite steel and concrete beams with welded sections), Kravanja et al. [3] (composite floor structures consisting of reinforced concrete slabs and steel beams), and Almeida and Carneiro [4] (steel–concrete composite bridges and reinforced concrete bridges).

The use of cellular beams in civil construction has increased over the last few years, as these beams offer improved structural performance without increasing the final mass. With the introduction of openings, new collapse modes emerge (Morkhade et al. [5], Sae-Long et al. [6,7]), and analysis under cyclic loads (Guo et al. [8]) or in fire situations (Oribi et al. [9]) is developed to better understand the structural performance of the beam and to identify and improve verification criteria for the structure. However, optimization studies applied to cellular beams have recently been developed, with the focus on better defining the optimal section geometries, as in the works of Da Silva and Lubke [10] and Aguiar et al. [11]. Similarly, optimization studies on cellular composite steel–concrete beams can be found in the works of Ramos and Alves [12] and Silva et al. [13].

Over the past few years, the use of slabs with embedded steel has become increasingly common in civil construction, as it avoids shoring and speeds up the construction process. Some recent works [14–19] have conducted experimental analyses to better understand the structure's behavior. On the other hand, Loureiro et al. [20] analyzed the application of optimization techniques to studies of steel deck slabs, aiming to assess the behavior of the formwork before concrete curing and to apply the Particle Swarm Optimization (PSO) algorithm. Teixeira et al. [21] proposed an optimization problem after curing the concrete and adding reinforcement to the slab, using different optimization algorithms. A comparative analysis with a manufacturer found that gains from adding reinforcement are substantial, with a low impact on final emissions. Silva et al. [22] proposed a multi-objective study of steel deck slabs in both the pre-curing and post-curing phases of concrete and concluded that the post-curing phase governs the entire optimization problem. However, studies analyzing the composite system composed of cellular beams and steel deck slabs are scarce in the literature.

The choice of an optimization algorithm for a given problem depends on the problem type: whether it has continuous or discrete variables, is constrained or unconstrained, and has one or several objective functions. In this scenario, the present work is classified as a discrete-variable, constrained, single-objective problem. To solve the problem, the Particle Swarm Optimization (PSO) algorithm proposed by Kennedy and Eberhart [23], coupled with the Adaptive Penalties Method proposed by Barbosa and Lemonge [24], was implemented, as it is well-suited to this type of problem. This choice was mainly due to the algorithm's good performance across different applications [25–30].

However, despite the literature presenting optimization studies of cellular beams [10,11] and composite cellular beams [12,13], studies considering the interaction between the cellular beam and the steel deck slab, where the final geometry of the slab is considered as a design variable in the optimization problem, are still scarce in the literature, thus motivating this work.

Given the above, this study aims to perform a parametric analysis of the optimization of composite cellular steel–concrete beams with steel deck slabs, evaluating the impact of treating the slab as a design variable compared with approaches based on manufacturer catalogs, with emphasis on minimizing CO_2 emissions. To achieve this, an optimization model with discrete variables and code-based constraints is developed, solved using the Particle Swarm Optimization (PSO) algorithm coupled with an adaptive penalty method. The study compares results from catalog-based slab configurations and from treating the slab as a design variable, assessing the influence of key parameters, such as span and loading, on optimal solutions and on material consumption and CO_2 emissions. The main contribution lies in addressing the lack of integrated optimization studies for composite cellular systems with steel deck slabs, quantifying the limitations of catalog-based approaches, and demonstrating their impact on structural and environmental performance. The design constraints follow the recommendations established by Lawson and Hicks [31], and the optimization problem is solved using Particle Swarm Optimization, proposed by Kennedy and Eberhart [23].

This work is divided into 4 sections, the first being the introduction. Section 2 presents the formulation of the optimization problem, including the design variables, materials, and search space, and a flowchart illustrating how the problem is coupled with the optimization algorithm. Section 3 presents the numerical analyses and discussions. Finally, Section 4 presents the conclusions, limitations, and future directions for advancing research.

2. Optimization Problem Formulation

2.1. Optimization Design Variables

The design variables initially consider the geometric and mechanical parameters associated with the steel beam itself, including the selection of the steel profile from the catalog (x_1) comprising 88 laminated profiles and 113 welded profiles; the yield strength (x_2); the diameter of the circular openings (x_3); the spacing between consecutive openings (x_4); and the height of the expanded section (x_5). In addition, variables related to the composite slab with a steel deck are considered, including the concrete thickness (x_6), the steel deck thickness (x_7), the slab concrete's compressive strength (x_8), and the slab reinforcement ratio (x_9). The adopted design variables are schematically illustrated in Figure 1, while the corresponding bounds considered in the optimization process are presented in Table 1.

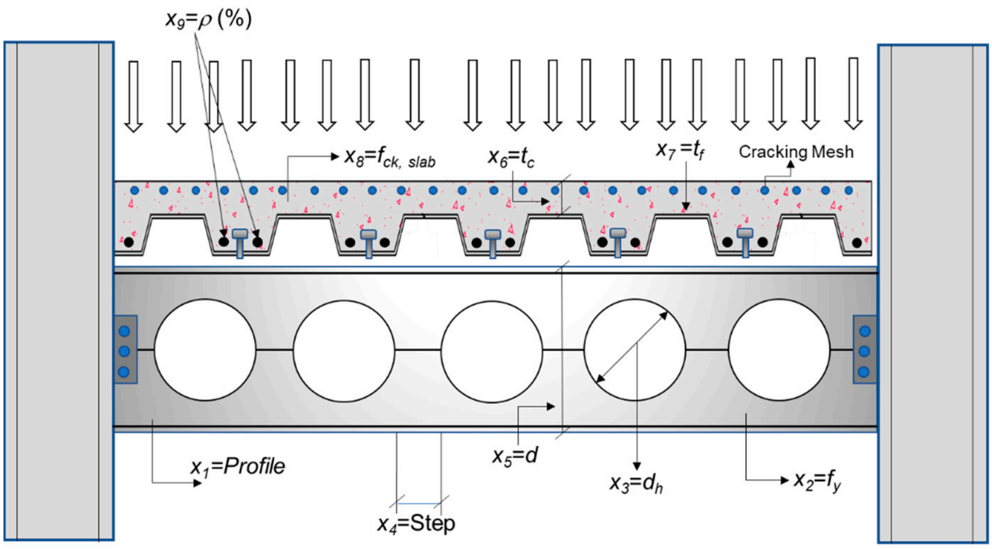

Figure 1. Design variables used in the optimization process.

Table 1. Design variables and optimization search space.

Design Variables	Search Space	Design Variables	Search Space
x_1 (Profile Choose)	[1:1:201]	x_6 (cm)	[50:5:80]
x_2 (MPa)	[345, 415, 455, 485]	x_7 (mm)	[0.80, 0.95, 1.25]
x_3 (Open Diameter)	[0.8:0.01:1.1]	x_8 (MPa)	[20:5:50]
x_4 (Step between opens)	[1.2:0.01:1.5]	x_9 (%)	[0.05:0.05:0.20]
x_5 (Expantion Factor)	[1.3:0.01:1.6]		

2.2. Objective Function

For the formulation of the optimization problem, the objective function was defined in terms of the CO_2 emissions of the composite structural system composed of cellular beams and steel deck slabs, as follows:

$$Min\ CO_2(kgCO_2) = CO_{2,steel} + CO_{2,cut} + CO_{2,weld} + CO_{2,formwork} + CO_{2,concrete} + CO_{2,connector} + CO_{2,crack,mesh} + CO_{2,reinf.mesh} \quad (1)$$

In Equation (1), CO_2 represents the carbon dioxide emissions associated with each component of the steel–concrete composite cellular beam, including the steel profile, cutting, welding, steel deck formwork, stud-bolt shear connectors, crack control mesh, and reinforcement mesh. The contribution of the steel profile is calculated as the structural mass of the profile multiplied by the emission factor of the selected steel. The cutting contribution corresponds to the total cutting length required to obtain the cellular section multiplied by the unit emission factor of the cutting process. The welding contribution is obtained by multiplying the total welding length required to fabricate the cellular beam by the unit welding emission factor, including any additional welding required to manufacture the steel profile, when applicable. The contribution of the steel deck formwork is determined from the deck mass per square meter multiplied by the emission factor of the steel used in the formwork. The concrete contribution is calculated from the volume of concrete in the slab multiplied by the emission factor of the selected concrete. Finally, the contributions of the shear connectors and the crack-control and reinforcement meshes are determined by multiplying the masses of these elements by their respective unit emission factors. For the determination of the emissions of each material, the unit parameters presented in Table 2 were adopted:

For the design constraints in beam dimensioning, the recommendations of Lawson and Hicks [31] were considered. For the steel-deck slab, the recommendations of NBR 8800:2024 [32] were used in conjunction with the work of Loureiro et al. [20] and Silva et al. [22]. Figure 2 presents a flowchart of the problem being addressed.

For the implementation of PSO to the analysis of the cellular composite beam problem, acceleration coefficients (c_1) and (c_2) equal to 2.05 were adopted, along with an inertia coefficient (w = 0.95).

Table 2. CO_2 Emissions of materials.

	Material	Units	CO_2 Emissions ($kgCO_2$,e)	Source
Concrete c(MPa)	25	m^3	374.00	Trentini et al. [33]
	30	m^3	394.11	
	35	m^3	416.12	
	40	m^3	438.09	
	50	m^3	486.19	

Table 2. *Cont.*

	Material	Units	CO_2 Emissions ($kgCO_2$,e)	Source
	Steel formwork	m^2	2.53	Negrin et al. [34]
	Reinf MeshABNT 1030	kg	2.01	
Steel (ASTM)	A572 Gr.50	kg	2.04	
	A572 Gr.60	kg	2.07	
	A572 Gr.65	kg	2.09	
	A913 Gr.65	kg	2.10	
	A913 Gr.65	kg	2.13	
	Cutting	m^2	20.09	
	Welding	m	0.03	

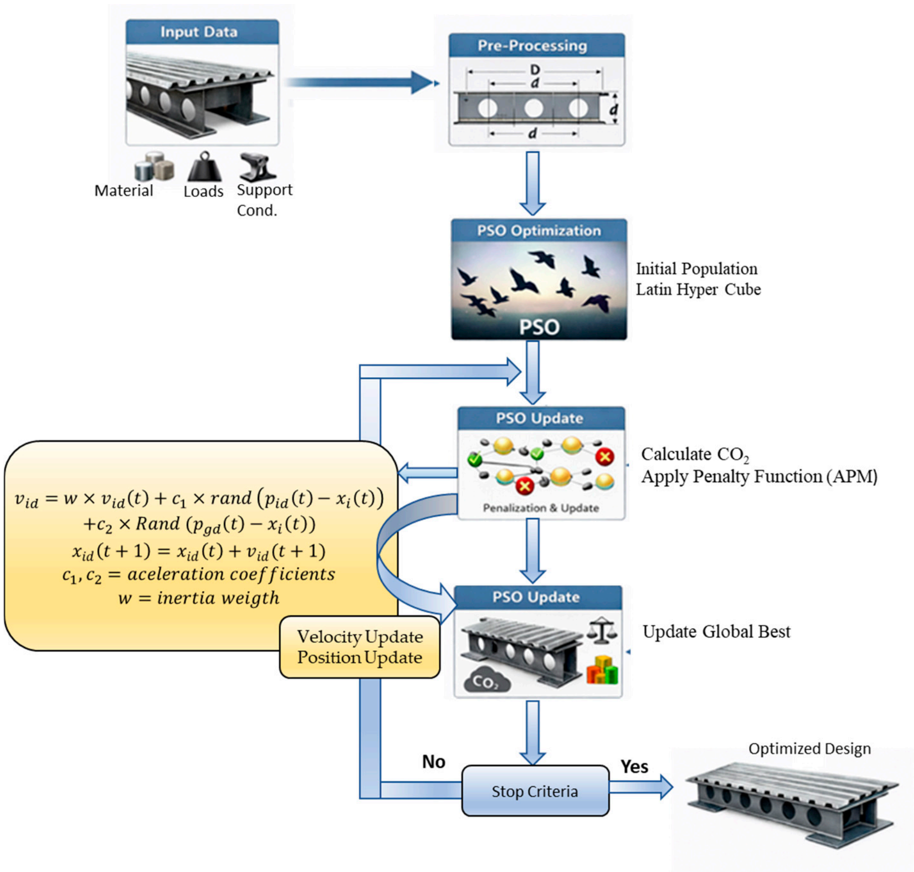

Figure 2. Flowchart of the optimization of composite cellular beams.

3. Numerical Results

The proposed formulation was evaluated in optimization scenarios for steel–concrete composite cellular beams, considering three distinct spans: 10 m to 20 m, with a step of 2.5 m. For each span, four steel-deck slab alternatives were analyzed, corresponding to slabs with widths of 3 m and 4 m, in optimized and non-optimized versions, subjected to live loads of 2 kN/m^2, 4 kN/m^2, and 6 kN/m^2. The actions considered in the model include the self-weight of the cellular beam and slab, construction loads of 1 kN/m^2, and dead load of 0.79 kN/m^2. The optimization process was carried out using the Particle Swarm Optimization (PSO), with the initial population generated through Latin Hypercube Sampling (LHS). A population of 100 individuals, 70 iterations, and 10 independent runs were adopted for each analyzed case, with structural constraints handled using the adaptive penalty method proposed by Barbosa and Lemonge [24]. The entire analysis and structural program, as well as the optimization algorithm, were implemented on the MATLAB 2020.a platform [35]. The convergence histories for the optimized slabs throughout the iterative process are presented in Figure 3 for the different load scenarios.

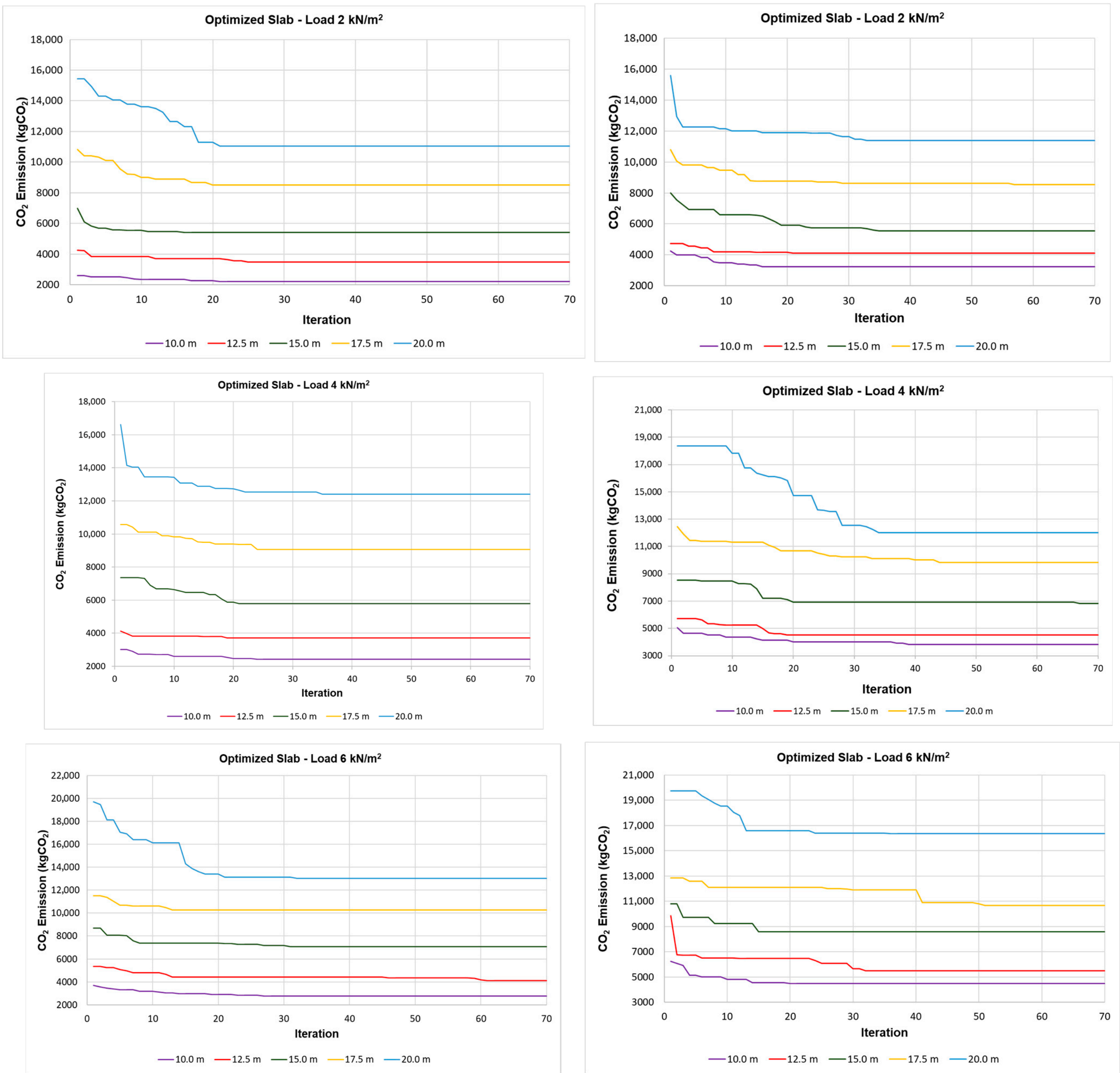

(**a**) Slab Span 3 m (**b**) Slab Span 4 m

Figure 3. Convergence history.

As observed, the algorithm demonstrates stable performance in all analyzed cases. Tables 3 and 4 present the final optimization results considering all evaluated scenarios, including the mean values of the objective functions, and Figure 4 illustrates the dispersion of the standard deviation across all analyzed scenarios, indicating the variability of the solutions.

Table 3. Final results for slabs with spans of 3 m.

Slab	Load (kN/m^2)	Span (m)	Profile	Steel (ASTM)	Steel Deck (*MF)	t_c (mm)	t_f (mm)	$f_{ck,slab}$ (MPa)	ρ (%)	CO_2 Emission ($kgCO_2$)	Media ($kgCO_2$)	Standard Deviation
Catalogue Slab	2	10.0	W 360 × 32.9	A572 Gr.50	50	50	1.25	25	0.00	2614	2633	1.9%
		12.5	W 460 × 52.0	A572 Gr.50	50	50	1.25	25	0.00	3762	3838	3.7%
		15.0	W 610 × 101.0	A572 Gr.50	50	50	1.25	25	0.00	6025	6025	0.0%
		17.5	VCS 750 × 120.5	A572 Gr.50	50	50	1.25	25	0.00	9205	9483	1.1%
		20.0	VCS 900 × 145.1	A572 Gr.50	50	50	1.25	25	0.00	11,523	12,247	4.1%
	4	10.0	W 410 × 38.8	A572 Gr.50	75	55	0.95	25	0.00	2786	2788	0.1%
		12.5	W 460 × 60.0	A572 Gr.50	75	55	0.95	25	0.00	4008	4139	1.2%
		15.0	W 610 × 101.0	A572 Gr.50	75	55	0.95	25	0.00	6086	6205	5.6%
		17.5	VCS 750 × 128.9	A572 Gr.50	75	55	0.95	25	0.00	9577	9682	2.5%
		20.0	VCS 950 × 170.5	A572 Gr.50	75	55	0.95	25	0.00	12,637	12,881	1.9%
	6	10.0	W 410 × 38.8	A572 Gr.60	75	55	1.25	25	0.00	3079	3138	2.3%
		12.5	W 530 × 66.0	A572 Gr.50	75	55	1.25	25	0.00	4500	4504	0.2%
		15.0	W 610 × 101.0	A572 Gr.50	75	55	1.25	35	0.00	6696	6951	4.0%
		17.5	VCS 800 × 150.7	A572 Gr.50	75	55	1.25	25	0.00	10,842	10,895	0.8%
		20.0	VCS 1000 × 182.9	A572 Gr.50	75	55	1.25	25	0.00	13,701	13,809	2.5%
Optimized Slab	2	10.0	W 360 × 32.9	A572 Gr.50	50	50	0.80	25	0.05	2214	2278	3.0%
		12.5	W 460 × 52.0	A572 Gr.50	50	50	0.80	25	0.05	3257	3418	5.0%
		15.0	W 610 × 101.0	A572 Gr.50	50	50	0.80	25	0.05	5414	5471	0.5%
		17.5	VCS 700 × 117.3	A572 Gr.50	50	50	0.80	25	0.20	8417	8778	2.0%
		20.0	VCS 900 × 145.1	A572 Gr.50	50	50	0.80	25	0.15	10,740	11,564	4.5%
	4	10.0	W 410 × 38.8	A572 Gr.50	50	55	0.95	25	0.20	2424	2487	2.2%
		12.5	W 530 × 66.0	A572 Gr.50	50	55	0.80	25	0.20	3695	3789	2.0%
		15.0	W 610 × 101.0	A572 Gr.65	50	55	0.80	25	0.20	5608	5728	0.9%
		17.5	VCS 750 × 128.9	A913 Gr.65	50	55	0.80	25	0.20	9070	9540	4.0%
		20.0	VCS 950 × 170.5	A572 Gr.50	50	65	0.80	25	0.15	12,125	12,443	1.8%
	6	10.0	W 410 × 38.8	A572 Gr.60	75	55	0.80	25	0.20	2655	2797	2.4%
		12.5	W 530 × 66.0	A572 Gr.50	75	55	0.80	25	0.20	3968	4033	1.0%
		15.0	W 610 × 101.0	A572 Gr.60	75	65	0.80	25	0.10	6058	6524	7.3%
		17.5	VCS 800 × 150.7	A572 Gr.50	75	60	0.80	25	0.10	10,170	10,340	1.0%
		20.0	VCS 1000 × 182.9	A572 Gr.50	75	55	0.80	25	0.20	12,849	13,061	1.8%

*MF—Steel-deck Metform Catalogue.

Table 4. Final results for slabs with spans of 4 m.

Slab	Load (kN/m^2)	Span (m)	Profile	Steel (ASTM)	Steel Deck (*MF)	t_c (mm)	t_f (mm)	$f_{ck,slab}$ (MPa)	ρ (%)	CO_2 Emission ($kgCO_2$)	Media ($kgCO_2$)	Standard Deviation
Catalogue Slab	2	10.0	W 360 × 32.9	A572 Gr.60	75	55	1.25	25	0.00	3699	3813	1.1%
		12.5	W 460 × 60.0	A572 Gr.50	75	55	1.25	25	0.00	5296	5369	1.5%
		15.0	W 610 × 101.0	A572 Gr.50	75	55	1.25	25	0.00	7649	7662	0.3%
		17.5	VCS 750 × 128.9	A572 Gr.50	75	55	1.25	25	0.00	11,400	11,427	0.5%
		20.0	VCS 950 × 170.5	A572 Gr.50	75	55	1.25	25	0.00	14,712	14,830	1.4%
	4	10.0	W 410 × 38.8	A572 Gr.60	75	95	1.25	25	0.00	4479	4612	1.0%
		12.5	W 530 × 66.0	A572 Gr.50	75	95	1.25	25	0.00	6250	6283	0.4%
		15.0	W 610 × 101.0	A572 Gr.50	75	95	1.25	25	0.00	8616	8681	1.3%
		17.5	VCS 800 × 150.7	A572 Gr.50	75	95	1.25	25	0.00	13,324	13,344	0.3%
		20.0	VCS 1000 × 182.9	A572 Gr.50	75	95	1.25	25	0.00	16,544	17,316	3.1%
Optimized Slab	2	10.0	W 360 × 39.0	A572 Gr.50	75	50	0.80	25	0.20	3178	3245	1.8%
		12.5	W 460 × 60.0	A572 Gr.50	75	50	0.80	25	0.20	4492	4620	1.8%
		15.0	W 610 × 101.0	A572 Gr.50	75	50	0.80	25	0.20	6666	6755	0.7%
		17.5	VCS 750 × 128.9	A572 Gr.50	75	50	0.80	25	0.20	10,257	10,541	2.8%
		20.0	VCS 950 × 170.5	A572 Gr.60	75	50	0.80	25	0.20	13,519	13,705	1.6%
	4	10.0	W 410 × 46.1	A572 Gr.50	75	65	0.95	25	0.20	3746	3824	1.8%
		12.5	W 530 × 66.0	A572 Gr.60	75	65	0.95	25	0.20	5191	5243	0.8%
		15.0	W 610 × 101.0	A572 Gr.60	75	65	0.95	25	0.20	7343	7739	6.6%
		17.5	VCS 750 × 128.9	A572 Gr.50	75	65	0.95	25	0.20	11,773	11,950	1.1%
		20.0	VCS 1000 × 182.9	A572 Gr.50	75	65	0.95	25	0.10	14,766	15,463	5.9%
	6	10.0	W 410 × 46.1	A913 Gr.60	75	105	0.80	25	0.20	4414	4600	2.5%
		12.5	W 530 × 66.0	A572 Gr.60	75	105	0.95	25	0.15	5782	6103	3.1%
		15.0	W 610 × 125.0	A572 Gr.50	75	105	0.95	25	0.15	8972	10,054	5.5%
		17.5	VCS 800 × 150.7	A572 Gr.60	75	105	0.80	25	0.20	12,678	12,905	1.2%
		20.0	VCS 1000 × 209.5	A572 Gr.50	75	75	1.25	25	0.20	16,907	19,305	9.9%

*MF—Steel-deck Metform Catalogue.

As shown in Table 5, for slabs with a span of 4 m, no feasible solutions were obtained when the manufacturer's catalog slab was used, as this span is the maximum allowable span specified by the manufacturer. According to Tables 4 and 5, the standard deviation for all solutions ranged from less than 1% to 9% for a span of 20 m and a load of 6 kN/m^2, up to the optimized slab. Figure 4 presents the interpolated response surface of these discrete results, showing a smooth variability between approximately 1% and 5%. These results demonstrate the algorithm's stability in finding solutions. It should also be noted that for spans up to 15 m, all solutions were obtained for rolled profiles across all load scenarios, whereas for spans beyond 15 m, they were obtained for welded profiles. This difference is mainly due to the fact that, in addition to the welding process used in the production of the cellular beam, the welding process used in the manufacturing of the profile itself was also included in the calculation of the welded profiles' emissions. An important point to note is the reduction in slab formwork thickness when reinforcement is added. These results corroborate those presented by Teixeira et al. [21] and Silva et al. [22], in which the slab formwork is one of the main components in the final structural designs for the composite beam-steel deck slab assembly. It is also observed that, in the vast majority of cases, the steels used in the solutions were ASTM A572 Gr.50, and the slabs had an f_{ck} of 25 MPa. For a 6 kN/m^2 load and a 4 m span, steel with a higher resistance grade was used. Figure 5 shows the ratio of solutions obtained with the optimized slab to those obtained with the catalog slab.

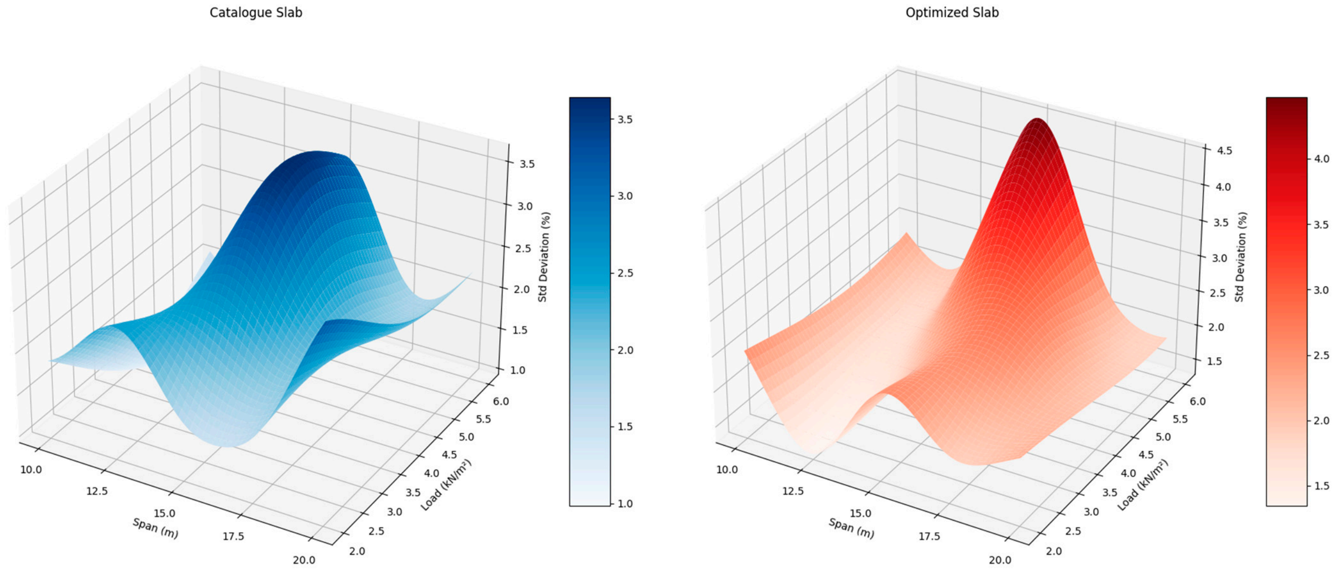

Figure 4. Standard deviation graphic.

Table 5. Final Beam Geometries to Load of 6 kN/m^2.

Span (m)	Slab Span: 3 m	Slab Span: 4 m
10.0	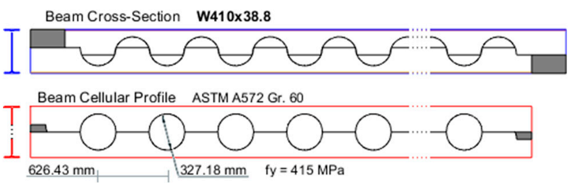	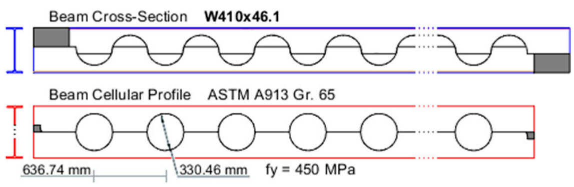
12.5	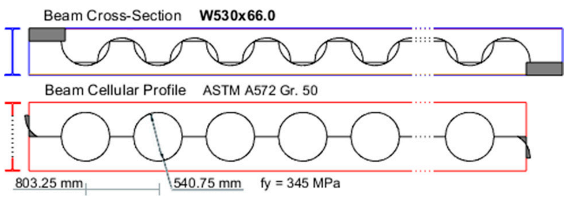	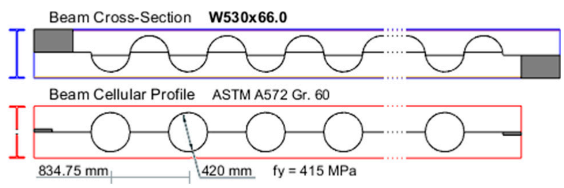

Table 5. *Cont.*

Span (m)	Slab Span: 3 m	Slab Span: 4 m
15.0	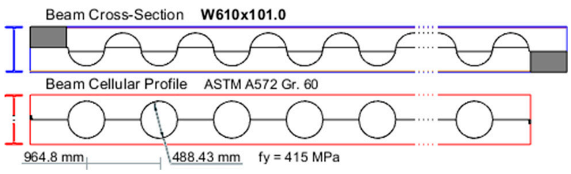	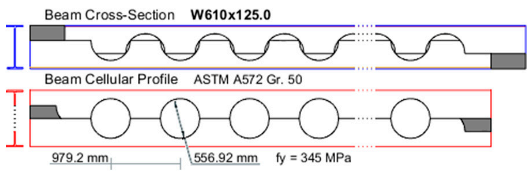
17.5	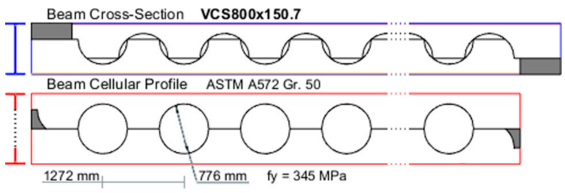	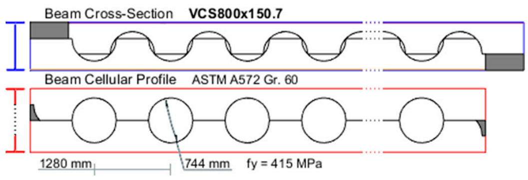
20.0	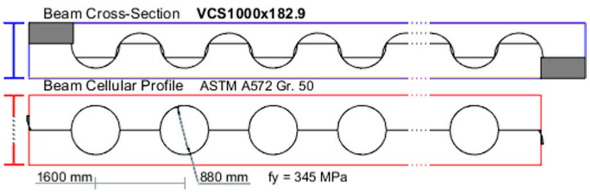	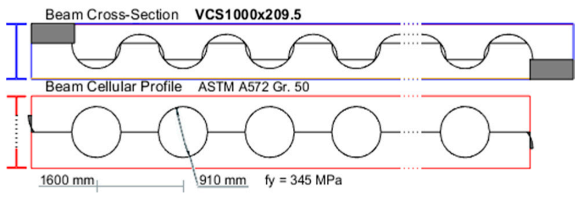

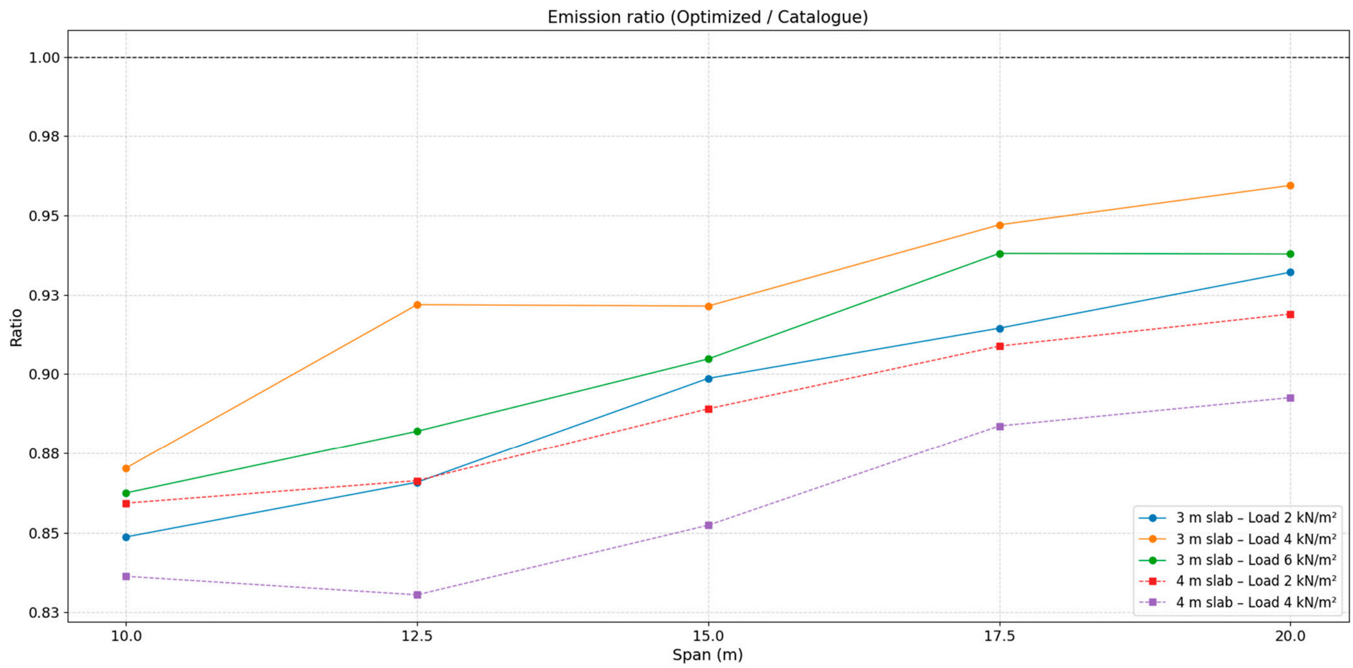

Figure 5. Ratio solutions between optimized and catalog slabs.

As shown in Figure 5, all scenarios in which the slab was considered as a design variable presented improved results compared with the catalog configuration, with emission reductions exceeding 17% in some cases. The influence of this parameter becomes more pronounced at higher load levels, particularly at 4 kN/m^2 and 6 kN/m^2, and for slabs with a span of 4 m. Figure 6 presents the evolution of CO_2 emissions per meter of beam for the different scenarios analyzed, considering a slab span of 3 m.

As shown in Figure 6 and confirming the trends observed in Figure 4, the use of optimized cellular beams combined with optimized steel-deck slabs results in lower CO_2 emissions for the structural system. This behavior is consistently observed across the different load levels and span lengths analyzed. For similar structural conditions, the optimized slab configuration consistently yields lower emissions than the catalog slab solution, as indicated by the displacement of the contour curves toward lower emission values. This demonstrates that treating the slab as a design variable significantly improves the structure's environmental performance. Furthermore, the results indicate that the influence of slab optimization becomes more pronounced as structural demands increase, particularly for larger spans and higher load levels, where material efficiency is more critical. Figure 7 presents the evolution of slab emissions considering a slab span of 4 m.

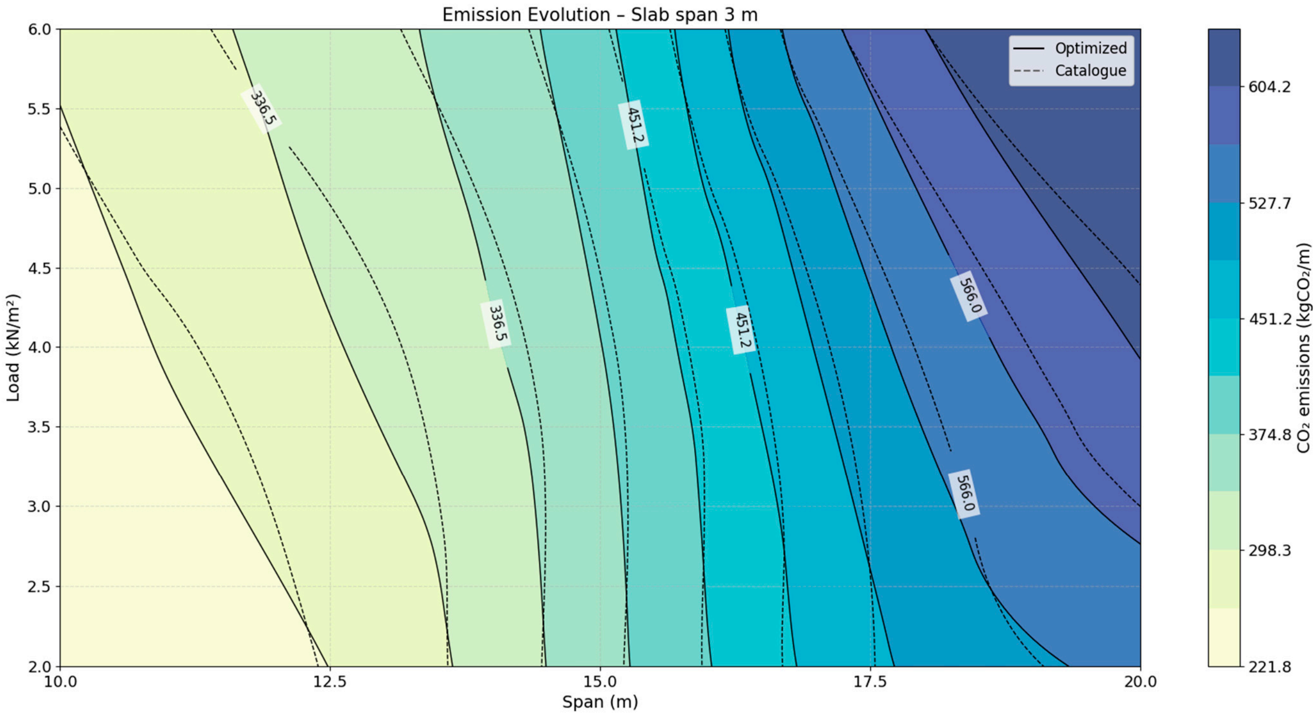

Figure 6. Analysis of the evolution of emissions.

As observed in Figure 6, the evolution of total CO_2 emissions follows a trend similar to that observed in Figure 5, increasing with both the structural span and the applied load level. This behavior is expected, since larger spans and higher loads require greater structural capacity, which generally results in increased material consumption. However, even under these more demanding structural conditions, the optimized solutions maintain improved environmental performance due to more efficient material distribution between the cellular beam and the steel-deck slab. Figure 8 presents the CO_2 emission composition, including material and variable contributions, for the final solution to the slab with a span of 3 m, for which all load cases were obtained.

According to Figure 8, the beam manufacturing process, including cutting and welding, and the welding process for the welded profiles, contribute very little to the structure's final emissions. These values highlight that, in addition to the gain in structural performance, where it is possible to achieve larger spans without adding structural mass, the beam production process is not an impediment. It can also be observed that the reduction in final emissions in the slab components when reinforcement is added contributed very low values to the final emissions of the structure. The graph shows the contribution of the 3 materials that most affect final emissions (steel profile, concrete, and steel deck), highlighting the need for research and proposals for innovative, environmentally friendly materials. Table 5 presents the final geometric configurations obtained for the optimized beams and slabs for the evaluated scenarios.

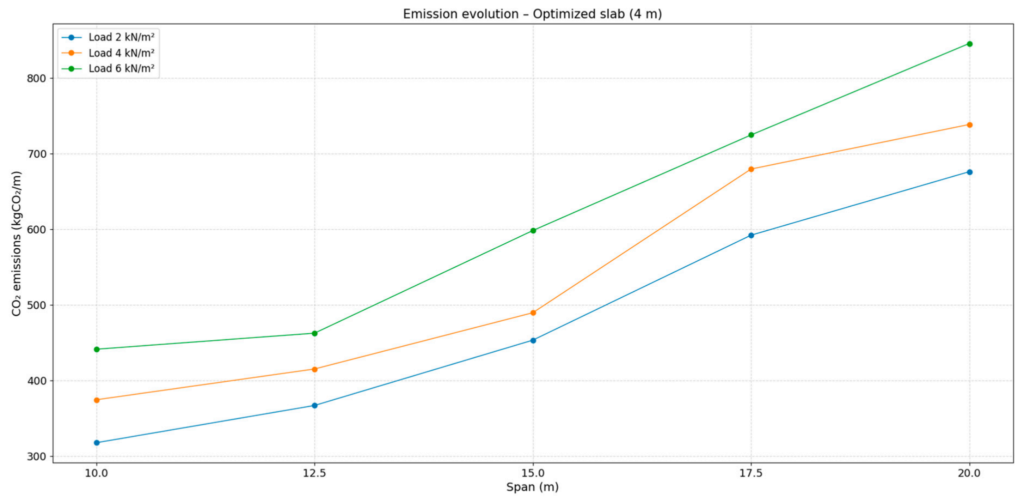

Figure 7. Analysis of the evolution of emissions to slab 4 m.

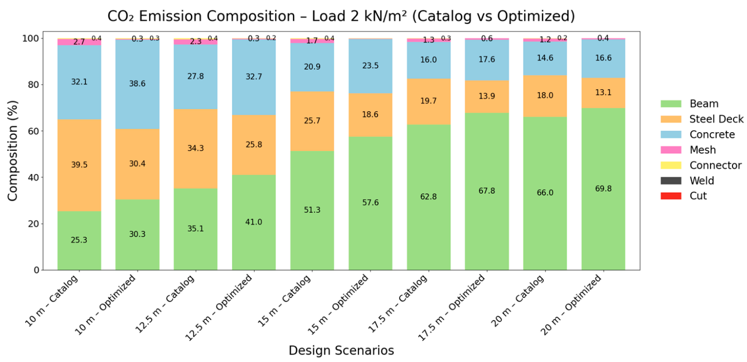

(**a**) Load 2 kN/m²

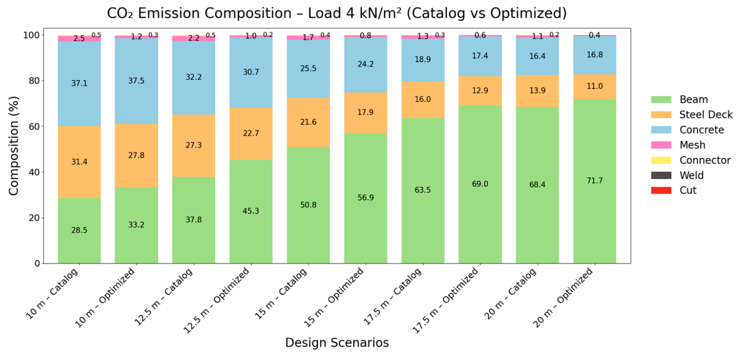

(**b**) Load 4 kN/m²

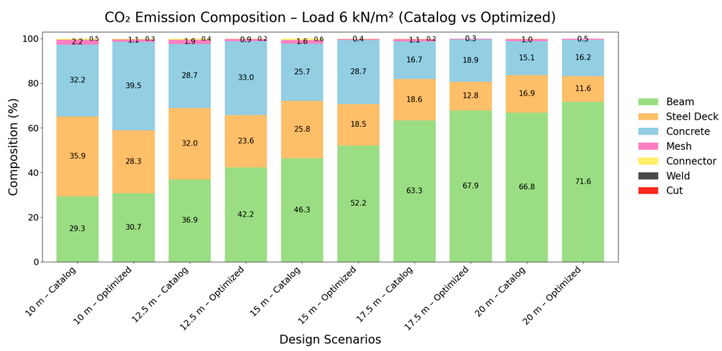

(**c**) Load 6 kN/m²

Figure 8. CO_2 emission composition.

4. Conclusions

This study achieved its main objective by performing a parametric analysis of the optimization of composite cellular steel–concrete beams with steel deck slabs, explicitly evaluating the impact of treating the slab as a design variable relative to conventional catalog-based approaches, with emphasis on minimizing CO_2 emissions.

The results demonstrated that the traditional use of manufacturer catalog slabs can significantly restrict the feasible design space, in some cases preventing the identification of viable structural solutions due to span and load limitations. In contrast, modeling the slab as a design variable enabled the exploration of a broader and more flexible solution space, leading to structurally feasible and environmentally superior designs.

From an environmental perspective, the proposed optimization approach proved highly effective, achieving CO_2 emission reductions exceeding 25% in certain scenarios. These improvements were primarily due to a more efficient redistribution of materials, enabled by the combined optimization of slab reinforcement, steel-deck thickness, and concrete topping thickness. The results also showed that the benefits of this approach become more pronounced for larger spans and higher loading conditions, highlighting the importance of integrated design strategies in demanding structural scenarios.

In terms of material selection, the optimization consistently favored solutions using ASTM A572 Grade 50 steel and 25 MPa concrete due to their lower emission factors and structural efficiency, although specific cases showed that slightly higher-impact materials may be justified when they lead to improved global system performance.

The study demonstrates that neglecting the slab as an active design variable can lead to suboptimal solutions, whereas its inclusion enables significant gains in both structural efficiency and environmental performance. This finding has direct practical implications, suggesting that designers should move beyond catalog-based approaches and adopt integrated optimization frameworks when aiming to reduce the carbon footprint of composite systems.

Finally, although the present study focused on cellular beams under standard loading conditions, the proposed methodology is general and can be extended to other beam typologies and design scenarios. Future work should explore multi-objective formulations that incorporate cost, serviceability, and dynamic performance and investigate structural behavior under fire conditions and alternative geometric configurations.

Author Contributions: Conceptualization, M.C.L.B., M.K. and É.C.A.; methodology, M.C.L.B., L.Y.-B., M.K. and É.C.A.; software, M.C.L.B. and É.C.A.; validation, M.C.L.B., L.Y.-B., M.K. and É.C.A.; formal analysis, M.C.L.B., L.Y.-B., M.K. and É.C.A.; investigation, M.C.L.B., L.Y.-B., M.K. and É.C.A.; data curation, M.C.L.B. and É.C.A.; writing—original draft preparation, M.C.L.B., L.Y.-B., M.K. and É.C.A.; writing—review and editing M.C.L.B., L.Y.-B., M.K. and É.C.A.; visualization, M.C.L.B., É.C.A.; M.K. and É.C.A.; project administration, É.C.A. All authors have read and agreed to the published version of the manuscript.

Funding: This research received no external funding.

Data Availability Statement: No datasets were generated or analyzed during the current study.

Acknowledgments: The authors acknowledge the funding agencies for their support in the development of this work. The first and fourth authors thank FAPES. The fourth author thanks FAPES for the postdoctoral fellowship (Grant Term No. 1134/2025-4), and the third acknowledges CNPq for the research grant (CNPq 305484/2023-0).

Conflicts of Interest: The authors declare no conflicts of interest.

Abbreviations

The following abbreviations are used in this manuscript:

PSO	Particle Swarm Optimization
$CO_{2,steel}$	CO_2 emission of steel
$CO_{2,cut}$	CO_2 emission of the cut profile
$CO_{2,weld}$	CO_2 emission of weld steel
$CO_{2,formwork}$	CO_2 emission of steel deck formwork
$CO_{2,concrete}$	CO_2 emission of concrete slab
$CO_{2,connector}$	CO_2 emission of the stud-bolt connector
$CO_{2,crack,mesh}$	CO_2 emission of crack mesh steel
$CO_{2,reinf.\ mesh}$	CO_2 emission of reinforcement mesh steel

References

1. United Nations Environment Programme. *Global Status Report for Buildings and Construction 2024/25: Towards a Zero-Emissions, Efficient and Resilient Buildings and Construction Sector*; UNEP: Nairobi, Kenya, 2024.
2. Tormen, A.F.; Pravia, Z.M.C.; Ramires, F.B.; Kripka, M. Optimization of steel-concrete composite beams considering cost and environmental impact. *Steel Compos. Struct.* **2020**, *34*, 409–421. [CrossRef]
3. Kravanja, S.; Klanšek, U.; Žula, T. Mass, direct cost and energy life-cycle cost optimization of steel-concrete composite floor structures. *Appl. Sci.* **2021**, *11*, 10316. [CrossRef]
4. Almeida, D.C.B.; Carneiro, A.M.P. Environmental impact of steel/concrete composite bridges and reinforced concrete bridges: A comparative analysis through life cycle assessment. *Ambient. Constr.* **2025**, *25*, e135202. [CrossRef]
5. Morkhade, S.G.; Jagtap, K.R.; Ghorpade, P.S.; Ahiwale, D.D.; Najm, H.M. Buckling performance evaluation of steel cellular beams strengthened with flange cover plate. *Asian J. Civ. Eng.* **2022**, *23*, 1277–1290. [CrossRef]
6. Sae-Long, W.; Arun, S.; Witthayapraphakorn, A.; Limkatanyu, S.; Damrongwiriyanupap, N.; Fakkaew, W.; Chaimahawan, P.; Thongchom, C. Local failure behavior of cellular beams: A parametric finite element study of web-post bending moment. *Results Eng.* **2026**, *29*, 109372. [CrossRef]
7. Sae-Long, W.; Arun, S.; Limkatanyu, S.; Chaimahawan, P.; Damrongwiriyanupap, N.; Fakkaew, W.; Wongchairattana, S. Behavior and design implications of web-post shear failure in cellular beams. *Results Eng.* **2025**, *27*, 106709. [CrossRef]
8. Guo, J.; Huo, S.; Zhao, H.; Li, T. Failure mechanism and load carrying capacity of hybrid high-strength steel composite cellular beams under low cyclic loading. *Buildings* **2025**, *15*, 3954. [CrossRef]
9. Oribi, S.B.; Kada, A.; Lamri, B.; Mesquita, L. Behaviour of cellular steel beams at ambient and high-temperature conditions. *J. Constr. Steel Res.* **2023**, *207*, 107969. [CrossRef]
10. Silva, A.R.; Lubke, G.P. Optimization of open web steel beams using the finite element method and genetic algorithms. *Structures* **2024**, *60*, 105785. [CrossRef]
11. Aguiar, L.A.; Monteiro, D.K.; Ceron, M.V.; Morsch, I.B. Optimum design of steel cellular beams using particle swarm optimization and finite element method. *Thin-Walled Struct.* **2025**, *215*, 113553. [CrossRef]
12. Ramos, J.R.S.; Alves, É.C. Numerical analysis of collapse modes in optimized design of alveolar steel-concrete composite beams via genetic algorithms. *REM Int. Eng. J.* **2021**, *74*, 173–181.
13. Silva, G.F.; Kripka, M.; Alves, É.C. CO_2 emission optimization of composite floor systems with cellular beams via metaheuristics algorithms. *Struct. Eng. Mech.* **2024**, *89*, 453–466.
14. Cifuentes, H.; Medina, F. Experimental study on shear bond behavior of composite slabs according to Eurocode 4. *J. Constr. Steel Res.* **2013**, *82*, 99–110. [CrossRef]
15. Ahmed, I.M.; Tsavdaridis, K.D. The evolution of composite flooring systems: Applications, testing, modelling and Eurocode design approaches. *J. Constr. Steel Res.* **2019**, *155*, 286–300. [CrossRef]
16. Grossi, L.G.F.; Santos, C.F.R.; Malite, M. Longitudinal shear strength prediction for steel-concrete composite slabs with additional reinforcement bars. *J. Constr. Steel Res.* **2020**, *166*, 105908. [CrossRef]
17. Celis-Imbajoa, E.I.; Paredes, J.A.; Bedoya-Ruiz, D. Experimental and analytical study at maximum load of composite slabs with and without conventional reinforcement applying the serial/parallel mixing theory and FEM. *Eng. Struct.* **2021**, *245*, 112700. [CrossRef]
18. Tian, J.; Wang, M.; Liu, J.; Guo, H.; Wang, Z.; Zhang, J. Experimental and numerical study of continuous span concrete composite slabs. *Structures* **2021**, *34*, 827–839. [CrossRef]
19. Shirgaonkar, A.A.; Patil, Y.D.; Patil, H.S. Longitudinal shear bond strength of profiled deck composite slab: An experimental and analytical investigation. *Mater. Today Proc.* **2022**, *65*, 1939–1945. [CrossRef]

20. Loureiro, M.C.; Alves, É.C.; Calenzani, A.F.G. Geometry optimization of steel formwork for steel-concrete composite slabs. *Structures* **2023**, *58*, 105395. [CrossRef]
21. Teixeira, M.O.; Alves, É.C.; Valle, J.P.S.O.; Calenzani, A.F.G. Design of simply supported composite slabs of steel and concrete via metaheuristic optimization algorithm. *Asian J. Civ. Eng.* **2023**, *25*, 237–252. [CrossRef]
22. Silva, I.O.M.; Alves, É.C.; Calenzani, A.F.G. Multiobjective optimization of steel and concrete composite slabs via MOPSO algorithm. *Structures* **2025**, *80*, 109722. [CrossRef]
23. Kennedy, J.; Eberhart, R.C. *Swarm Intelligence*; Morgan Kaufmann: Burlington, MA, USA, 2001. [CrossRef]
24. Barbosa, H.J.C.; Lemonge, A.C.C. An adaptive penalty scheme in genetic algorithms for constrained optimization problems. *GECCO Proc.* **2002**, *2*, 287–294.
25. Barroso, E.S.; Parente, E.; Melo, A.M.C. A hybrid PSO-GA algorithm for optimization of laminated composites. *Struct. Multidiscip. Optim.* **2017**, *55*, 2111–2130. [CrossRef]
26. Mokarram, V.; Banan, M.R. A new PSO-based algorithm for multi-objective optimization with continuous and discrete design variables. *Struct. Multidiscip. Optim.* **2018**, *57*, 509–533. [CrossRef]
27. Biabani, F.; Shojaee, S.; Hamzehei-Javaran, S. A new insight into metaheuristic optimization method using a hybrid of PSO, GSA, and GWO. *Structures* **2022**, *44*, 1168–1189. [CrossRef]
28. Mahapatra, A.K.; Panda, N.; Pattanayak, B.K. Hybrid PSO (SGPSO) with discretization operator for training RBF neural network and optimal feature selection. *Arab. J. Sci. Eng.* **2022**, *48*, 7059–7075. [CrossRef]
29. Tong, F.; Yang, J.; Ma, C.; Cheng, L.; Li, G. Prediction of concrete dam displacement using Copula-PSO-ANFIS hybrid model. *Arab. J. Sci. Eng.* **2022**, *47*, 4335–4350. [CrossRef]
30. Shao, J.; Fan, Z.; Huang, Y.; Zhan, Y.; Cai, Q. Multi-objective optimization of double-walled steel cofferdams based on RSM and PSO algorithm. *Structures* **2023**, *49*, 256–266. [CrossRef]
31. Lawson, R.M.; Hicks, S.J. *Design of Composite Beams with Large Web Openings: In Accordance with Eurocodes and the UK National Annexes*; SCI: London, UK, 2011.
32. Associação Brasileira de Normas Técnicas (ABNT). *NBR 8800: Design of Steel and Composite Steel–Concrete Structures for Buildings*; ABNT: Rio de Janeiro, Brazil, 2024. (In Portuguese)
33. Trentini, E.V.W.; Parsekian, G.A.; Bittencourt, T.N. Multiobjective optimization of bridge and viaduct design: Comparative study of metaheuristics and parameter calibration. *Eng. Struct.* **2024**, *312*, 118252. [CrossRef]
34. Negrin, I.; Kripka, M.; Yepes, V. Design optimization of a composite typology based on RC columns and THVS girders to reduce economic cost, emissions, and embodied energy of frame building construction. *Energy Build.* **2025**, *336*, 115607. [CrossRef]
35. MathWorks. *MATLAB*®, R2021a; MathWorks Inc.: Natick, MA, USA, 2020.